JOURNAL OF GEOPHYSICAL RESEARCH, VOL. 105, NO. A8, PAGES 18,857–18,866, AUGUST 1, 2000

Statistical study of auroral kilometric radiation fine structure striations observed by Polar

J. D. Menietti, A. M. Persoon, J. S. Pickett, and D. A. Gurnett

Department of Physics and Astronomy, University of Iowa, Iowa City

Abstract. We have conducted a statistical survey of a semirandom sample of the auroral kilometric radiation (AKR) data observed by the plasma wave instrument wideband receiver on board the Polar spacecraft. We have determined that AKR fine structure patterns with very narrowband, negative drifting striations occur in approximately 6% of the high-resolution wideband spectrograms when AKR is present. Positive sloping striations are also observed, but at a much lower rate. More than 8200 AKR stripes have been scaled. The stripes are predominantly found in the 40- to 215-kHz frequency range and have a frequency extent of about 4 kHz and a duration of usually less than 2 s. The majority of the stripes have drift rates between -8 and -2 kHz/s, with a peak in the distribution between -6 and -4 kHz/s. There is also a much smaller group of striations with positive drift rates of up to about 5 or 6 kHz/s. We have further investigated the change of drift rate with frequency. Almost all striations are observed in the lowest two frequency bands of the wideband receiver ($f < 215$ kHz). There is an increase in the statistical drift rate with increasing frequency. The statistical slope of the striations increases with frequency from about -4.4 kHz/s at 75 kHz to about -5.7 kHz/s at 170 kHz. This frequency dependence of the drift rate is consistent, under certain conditions, with a production mechanism stimulated by an upward propagating electromagnetic ion cyclotron wave, as had been suggested earlier. However, such a changing drift rate is also compatible with a stimulated source region that propagates upward along the magnetic field line at the velocity of an ion beam accelerated by a local, upward directed electric field, as is typically observed in the auroral region. An explanation for this association is not apparent at this time.

1. Background

Gurnett et al. [1979] and *Gurnett and Anderson* [1981] using ISEE data, *Benson et al.* [1988] using DE 1 data, and *Morioka et al.* [1981] using Exos-B data have all reported examples of auroral kilometric radiation (AKR) fine structure in both the ordinary and extraordinary modes, indicating that AKR is emitted in discrete bursts lasting only a few seconds or less. Observed frequency drift rates of features are in the range from $R > 100$ Hz/s to $R <$ tens of kilohertz per second. The bandwidth can be quite small (<1 kHz). *Gurnett et al.* [1979] suggest that the drifting features may be due to rising and falling source regions. The fine structures include not only drifting features, but also discrete bands of near-monochromatic emission and other discrete features that are seen at the highest resolution available. Auroral roar is a relatively narrowband emission occurring near twice the electron gyrofrequency and was first detected by *Kellogg and Monson* [1979]. *LaBelle et al.* [1995] and *Shepherd et al.* [1997, 1998] have reported similar structures in auroral roar emissions at frequencies of a few megahertz (2 or 3 times the local gyrofrequency). The signatures include a series of "multiple discrete features" with positive slope on a frequency-time spectrogram. These signatures are similar to those described by *Menietti et al.* [1996] in the AKR fine structure as "stripes" and postulated as stimulated emission. We consider these stripes or striations a unique class or subset of AKR fine structure. A strict definition is difficult to formulate, but as described by *Menietti et al.* [1996] these striations appear as narrow, discrete stripes on a frequency-time spectrogram, as if one were to scratch the surface of the spectrogram with a sharp needle or comb. Since they have a unique appearance among the array of fine structure signatures, we postulate they may have a unique source. The relationship, if any, between the auroral roar discrete signatures and the AKR stripes is not known. We point out a similarity between these striation observations and Jovian "S-bursts" observed at higher frequency both by the Voyager spacecraft and by ground-based telescopes [*Carr et al.*, 1983, 1997; *Zarka et al.*, 1996]. This similarity has been suggested in the past by *Shepherd et al.* [1998].

There are a number of theories which attempt to explain the source of the AKR fine structure observed. Such knowledge is necessary if we are to fully understand the details of the AKR generation mechanism. *Wu and Lee* [1979] have no doubt identified the general instability mechanism responsible for the emission, but as pointed out some years ago by *Melrose* [1986], the cyclotron maser mechanism would be an incomplete theory if it could not explain the timescales of wave growth associated with AKR fine structure.

Calvert [1982] has proposed that AKR fine structure can be explained by a feedback model, which requires radiation oscillations (similar to an optical laser) in a density enhancement region of diameter $\lesssim$25 km that converges with altitude. The source would emit radiation at its normal modes and would thus naturally explain monochromatic fine structure bands. Fine structure features that are observed to drift in frequency are explained in the feedback model by density gradients at the boundaries of the density enhancement region. *Melrose* [1986] has proposed a feedback model that depends on a phase-bunching mechanism and the wave-trapping

Paper number 1999JA000389.
0148-0227/00/1999JA000389$09.00

saturation model of VLF emission growth put forth by *Helliwell* [1967]. Melrose's theory of AKR fine structure depends critically on the assumption that the particle-wave interaction region for AKR growth has a parallel velocity intermediate between those of the particles and the waves.

Occasional monochromatic signatures including bands of emission have been observed in the AKR fine structure. *Grabbe* [1982] presents examples of the latter features which he explains in terms of a three-wave generation mechanism based on ion cyclotron waves [*Grabbe et al.*, 1980]. *Farrell* [1995] has recently suggested that some monochromatic features in the AKR fine structure can be explained by free-energy electrons interacting with an oscillating density cavity boundary that has quasi-monochromatic wave-like motion. Adiabatic changes in the structure of the cavity can lead to drifting radio tones similar to those observed.

McKean and Winglee [1991] have performed one-dimensional P-I-C (particle-in-cell) simulations of AKR fine structure from sources associated with strong magnetic field gradients due to currents thought to be near or along the source field line. These authors find that rapidly drifting features (>10 kHz/s) are proportional to the growth rate (for positive drift rate) or nearly constant (for negative drift rate). For slowly drifting features (close to observed drifts) the rates are approximately proportional to the B-field gradient. Most recently, *Yoon and Weatherwax* [1998] have performed numerical calculations of AKR growth rate using more realistic electron distribution functions. In contrast to past work with loss-cone, ring-beam, or Dory-Guest-Harris (DGH) distributions, Yoon and Weatherwax relied on the observations of the Fast Auroral Snapshot (FAST) satellite observations in the auroral AKR source region [cf. *Ergun et al.*, 1998b; *Delory et al.*, 1998]. They obtain narrow bandwidths of the order of $\Delta f/f \sim 10^{-3}$. *Pritchett et al.* [1999] have conducted two-dimensional electromagnetic particle simulations also using electron distributions based on FAST observations to obtain similar intrinsic bandwidths of AKR in the source region (~0.5-1.0 kHz). Understanding the source of AKR fine structure is critical to understanding details of the generation mechanism. The bandwidth of the fine structure, for instance, puts severe constraints on spatial growth rates as produced by the cyclotron maser instability.

As mentioned above, *Menietti et al.* [1996], in trying to explain a unique class of AKR fine structure referred to as striations, have presented observations of possible stimulated AKR. In Menietti et al.'s paper, impulsive wave generation and intrinsic velocity dispersion were discounted as possible sources of the discrete signatures observed in the wave data. *Menietti et al.* [1997] extended that work by presenting additional observations of the phenomena observed by Polar and presented a scenario for the generation of negative- and positive-slope signatures. *Menietti et al.* [1997] suggested that the negative-slope stripes are produced by stimulation of the source region by electromagnetic plasma waves traveling away from Earth, through the AKR source region. A wave traveling up the magnetic field line with a group velocity of about 1000 km/s would pass through the AKR source region (40 kHz $< f <$ 65 kHz) in about 3.5 s, in agreement with the typical observations. The source of the upward propagating electromagnetic ion cyclotron (EMIC) waves may be near the top of the acceleration region where upward electron beams are more common than precipitating electron beams. Alternatively, the EMIC source region could extend below the acceleration region, in which case downward EMIC waves, which subsequently reflect at low altitude to propagate back up through the AKR source region, might be the source of the AKR stripes. Positive-slope stripes, alternatively, could be stimulated by downward propagating EMIC waves. These waves may be associated with AKR that propagates principally toward the Earth and thus is not typically observed by a satellite above the AKR source region.

AKR has been observed by the Polar plasma wave instrument (PWI) on almost every Northern Hemisphere pass. High-resolution frequency-time spectrograms obtained by the PWI wideband receiver sometimes show discrete, negative drifting striations, each extending over a period of several seconds. Often occurring in packets and occasionally in isolation, these AKR stripe-like striations appear to have a linear frequency drift on the frequency-time spectrograms and exhibit a very narrow bandwidth compared with other discrete features in the AKR spectrum. In this paper we present the results of a survey of striations observed by the Polar satellite plasma wave instrument. Statistics including frequency extent and drift rate are presented. The results call into question the proposal of EMIC waves as the stimulated source of the striations.

2. Instrumentation

The Polar satellite was launched in late February 1996 into a polar orbit with an apogee of about 9 R_E and a perigee of about 1.8 R_E. Polar is the first satellite to have three orthogonal electric antennas, three triaxial magnetic search coils, and a magnetic loop antenna, as well as an advanced plasma wave instrument [*Gurnett et al.*, 1995]. This combination can potentially provide the polarization and direction of arrival of a signal without any prior assumptions.

The plasma wave instrument on the Polar spacecraft is designed to provide measurements of plasma waves in the Earth's polar regions over the frequency range from 0.1 Hz to 800 kHz. Five receiver systems are used to process the data: a wideband receiver, a high-frequency waveform receiver, a low-frequency waveform receiver, two multichannel analyzers, and a pair of sweep frequency receivers. For the high-frequency emissions of interest here, the wideband receiver (WBR) is of special importance. This receiver provides high-resolution waveform data and is programmable, allowing the selection of 11-, 22-, or 90-kHz bandwidths with a lower band edge (base frequency) at 0, 125, 250, and 500 kHz.

3. Observations: The Survey

We have conducted two surveys of the PWI plasma wave wideband (high resolution) receiver data. In survey 1 we randomly sampled wideband data during the entire first year of Polar operations. Since this survey included only a very small sample of data for $f >$ 90 kHz, a second comprehensive survey of data was conducted during the first week of Polar operations, when PWI cyclically sampled emissions over its entire frequency range. In the surveys which we report, there are a number of possible sources of error. Measurements were performed on individual stripes by setting computer crosshairs on the signatures as they appear on a spectrogram. Some striations were more difficult than others to measure due to contrast with background emission. For any particular measurement, there is error in positioning the crosshairs. We deem these errors to be statistically small due to the large sample size, but typically less than 1% per measurement.

Plate 1 is a 48-s frequency-time spectrogram taken from the wideband data for March 1, 1997, starting at 1618:25 UT, when the wideband receiver was operating with a bandwidth of 90 kHz and a base frequency of 0 kHz. At this time the spacecraft is located over the polar cap at a radial distance of about 8.6 R_E, well above the AKR source region. This spectrogram illustrates a typical striation pattern in the AKR spectrum from 40 to 90 kHz. Many of these stripes are very intense. Some are clearly identified when the intensity of the stripes exceeds the background AKR spectral intensity or they occur below the diffuse AKR spectrum. All of these stripes have a negative drift rate. Striation patterns such as

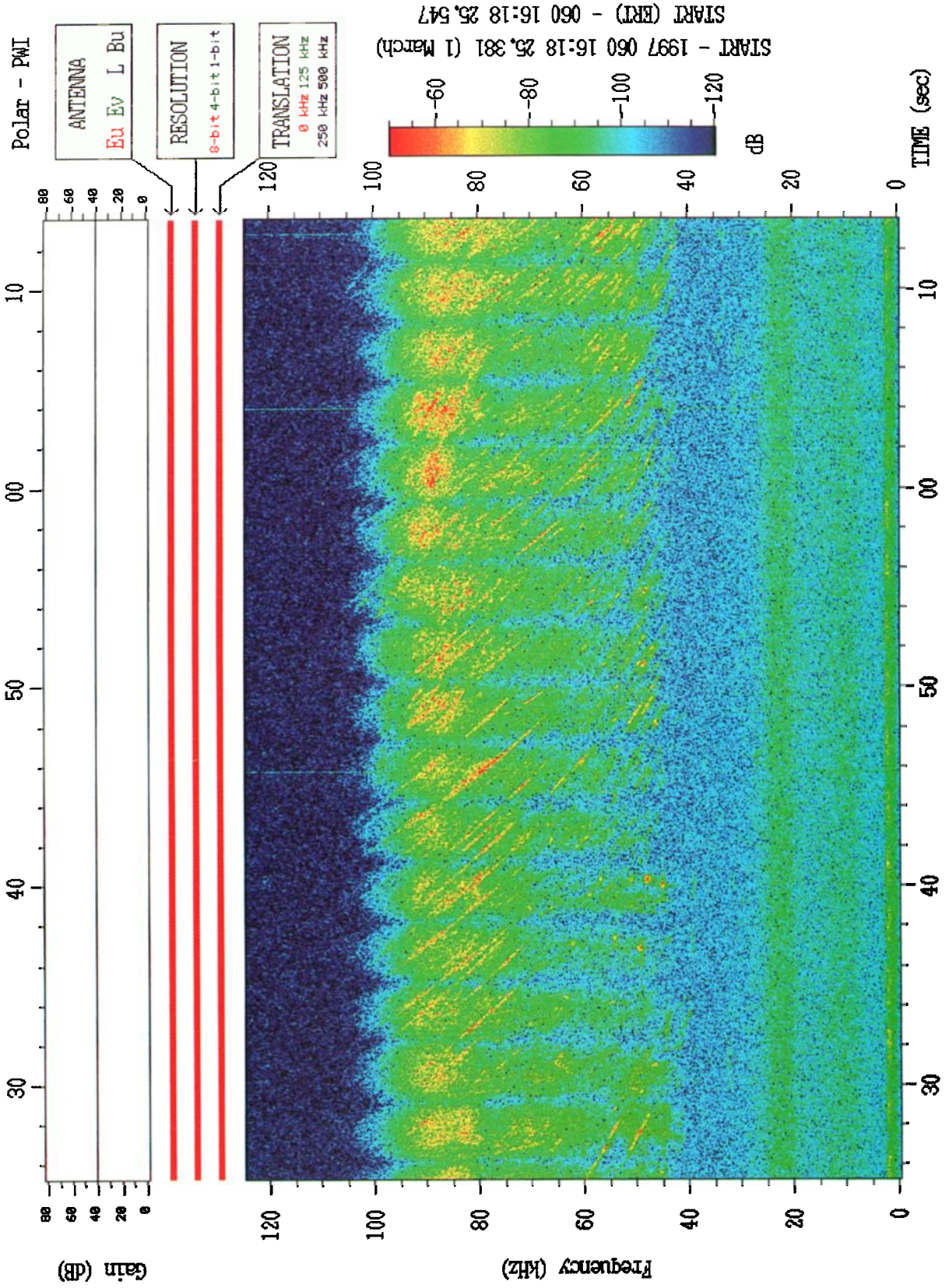

Plate 1. A 48-s frequency-time spectrogram taken from the wideband data for March 1, 1997, starting at 1618:25 UT. At this time the spacecraft is located over the polar cap, well above the auroral kilometric radiation (AKR) source region.

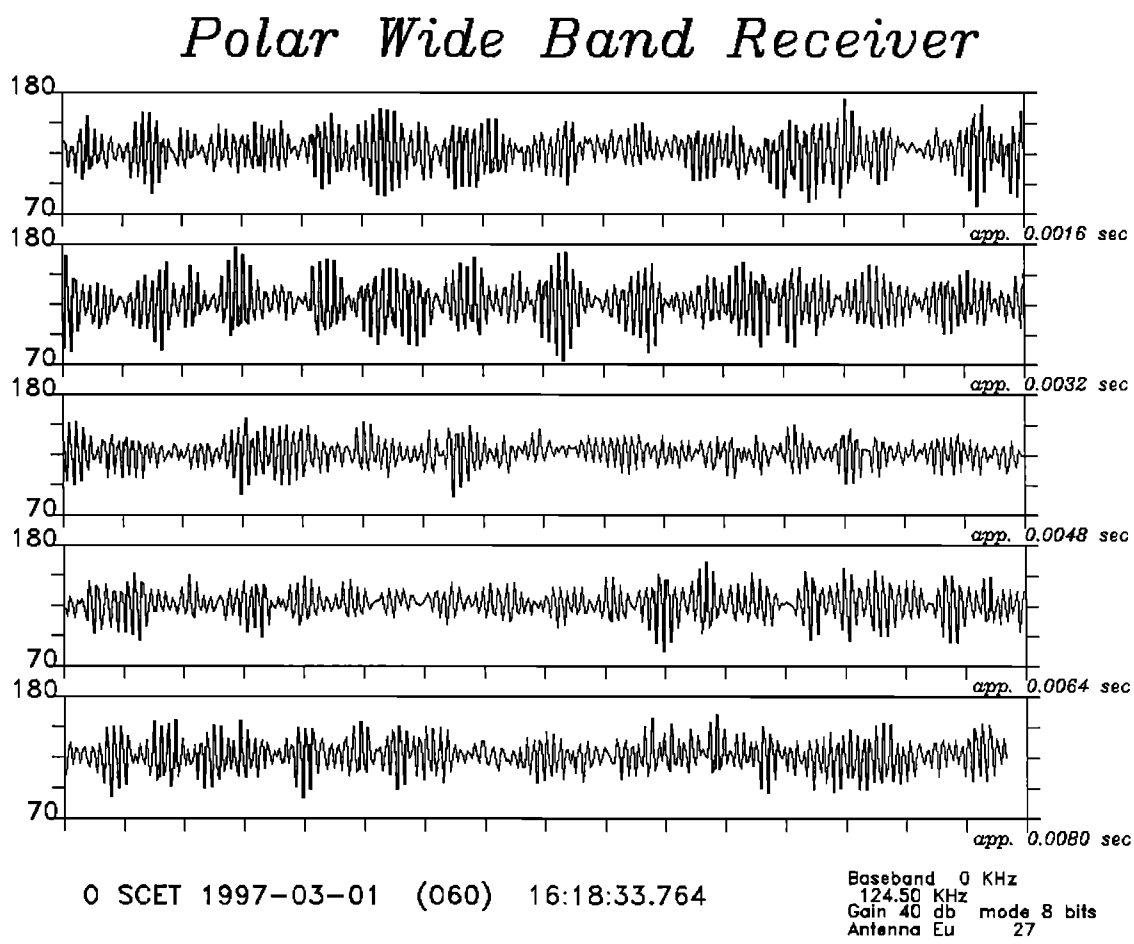

Figure 1. A plot of the waveform (arbitrary units) versus time. The start time of the plot is 1618:33.764 UT and each panel spans 0.0016 s. Note the oscillation at ~80 kHz and the modulation of the signal.

these were found nearly continuously for more than an hour of wideband data beginning at 1559 UT on this date.

In Figure 1 we display the waveform data for a small portion of the period shown in Plate 1 beginning at the time 1618:33.764 UT. The waveform is in arbitrary units proportional to the electric field strength. One panel corresponds to only 1.6×10^{-3} s. Clearly seen in each panel is a dominant oscillation occurring in wave packets or bursts, with a frequency close to 80 kHz. There is also a much slower modulation of this higher frequency, which may be due to a beating of two or more closely spaced striations detected at this time. An alternative explanation for this modulation is that it occurs for each striation and is due to independent wave growth or amplification centers with similar, but slightly different frequencies and random phases and amplitudes. This suggestion has been made to explain the very similar waveforms observed for Jovian S-bursts at higher frequency [cf. *Carr and Reyes*, 1999]. This plot thus demonstrates that the striations observed in Plate 1 are not artifacts of a Fourier transform (necessary to obtain the spectrogram of Plate 1) and that the source mechanism may require a certain impulsiveness or randomness. A subsequent plot of the waveform, less than 1 s later (not shown), shows a measurably decreased frequency as observed in Plate 1.

Altogether, in survey 1, 38.6 hours of wideband data were surveyed to record occurrences of similar AKR striation patterns. The orbit coverage of the data set is displayed in the polar plot of invariant latitude versus magnetic local time (Plate 2). For 87.6% of the 90-kHz bandwidth data the instrument was sampling with a base frequency of 0 kHz (i.e., with a bandwidth in the frequency range $0 < f < 90$ kHz). For most of the remainder of the time, the base frequency was 125 kHz ($125 < f < 215$ kHz). During the first year of wideband operations, the 90-kHz bandwidth data were most frequently acquired at high auroral and polar latitudes in the Northern Hemisphere. The semirandom survey 1 yielded 8300 s of AKR striation data, which is approximately 6% of the 90-kHz bandwidth data taken. There were 98 occurrences of contiguous striation patterns, most of them lasting less than 2 min.

To quantitatively estimate the width in frequency of an isolated stripe, we chose an episode with few, well-separated stripes on April 1, 1996. Two stripes were seen in the frequency range from 75 to 90 kHz. Starting with the waveform data (antenna response versus time), we performed a fast Fourier transform using a Hanning smoothing window to reduce noise. The result of this analysis was a plot of the power spectral density versus time from which we estimate the width of an individual stripe to be $\Delta f/f \sim 4 \times 10^{-3}$. For a frequency near 75 kHz this yields a width in frequency of about 300 Hz. This measured thickness is at the limit of resolution due to the sampling rate and operating mode of the instrument and a 25% duty cycle. We acknowledge that the actual frequency width of an individual stripe may be much less.

Survey 1 provided a good sampling of the radio emission data during the first year of operations, but except for the first few weeks, the plasma wave wideband receiver was almost always selected to monitor emissions in the frequency range from 0 to 90 kHz. In order to investigate the frequency dependence of the

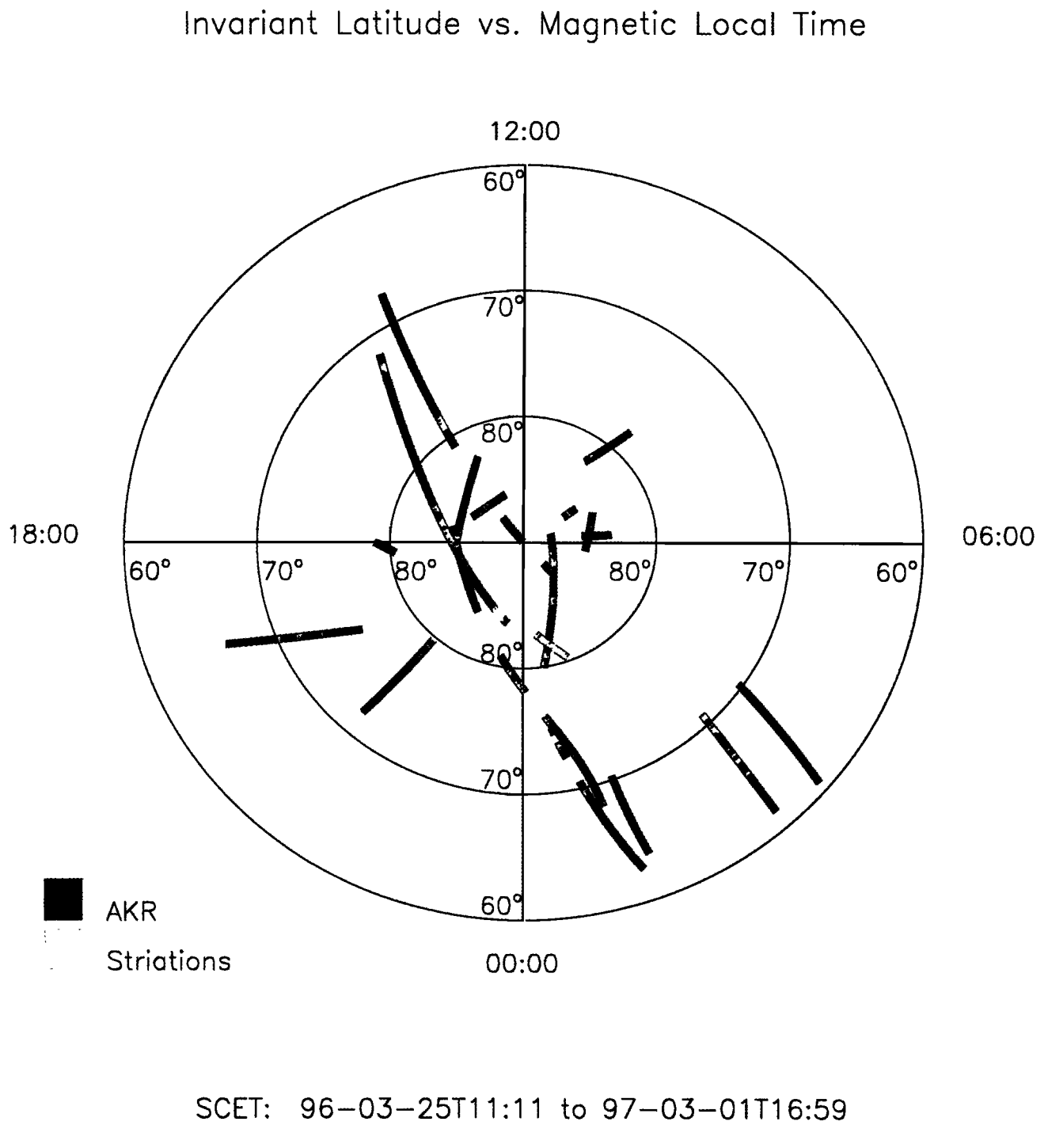

Plate 2. Orbit coverage of the data set displayed as a polar plot of invariant latitude versus magnetic local time.

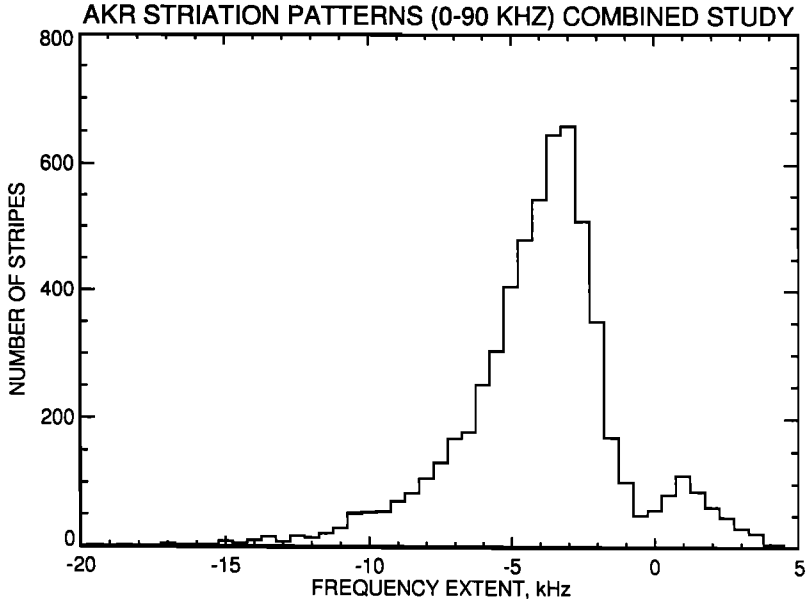

Figure 2. Frequency extent of the striations seen in the 0- to 90-kHz data for study 2. The data have been grouped in bins with a bandwidth of 0.5 kHz and displayed for all values of up to 20 kHz. The negative (positive) values of the coordinate refer to striations with decreasing (increasing) frequency as a function of time.

striations, a second survey was necessary. Survey 2 was conducted during the first week of PWI operations when the wideband receiver was cycled through all of its frequency bands.

To quantitatively determine the frequency drift, duration, and drift rate of the individual stripes in survey 2, more than 6200 striations at frequencies up to 590 kHz were scaled using a digitization technique. The scaling technique was used on about 51% of the 48-s wideband spectrograms showing striation patterns. While the scaling technique is very useful for accumulating a statistical database of AKR striations, it favors more intense stripes and isolated stripes that can be distinguished clearly from background noise and the diffuse AKR spectrum.

To examine the frequency extent of the striations (the total range in frequency of a particular stripe), we have combined the data from survey 1 and survey 2. In Figure 2 the data have been grouped in bins with a bandwidth of 0.5 kHz and displayed for all values with a frequency extent in the range $-20 < f < 5$ kHz, where negative frequencies are used for striations decreasing in frequency with time. The negative slopes have a frequency extent distribution that peaks at about -3.5 kHz, while the positive-slope striations have a distribution that peaks at only about 1 kHz. In Figure 2 we only display the results for $f < 90$ kHz. The results for $125 < f < 215$ kHz are qualitatively similar, but there is too little data for $f > 215$ kHz.

The total time duration of the striations was also calculated using data from the combined survey 1 and survey 2. Figure 3a clearly shows that most of the striations have a duration of less than 2 s, with a pronounced peak in the duration distribution between 0.5 and 1 s. The dropout in the distribution below 0.5 s is due, in part, to the limitations of the scaling technique. The number of striations with a positive slope is much less (Figure 3b), but the plot is qualitatively the same.

Figures 4a-4c illustrate the distribution of the frequency drift rates of the AKR striations as determined from survey 2 only. We have further segmented the data according to frequency range: 0-90 kHz (Figure 4a) and 125-215 kHz (Figure 4b). The data have been grouped in bins of 0.5 kHz/s. Because of the larger sampling times, most stripes are observed in the lowest frequency range. Each panel of Figure 4 shows a large peak for negative slope and a smaller peak for positive-slope striations. The number of striations found at the highest frequencies (Figure 4c) are far fewer, and the relative number of positive-slope striations is higher. Admittedly, the statistics for the highest frequencies are not as reliable. Superimposed on each curve of negative drift rates is a fit to a drifting Gaussian (solid curve) from which the best-fit drift rate is obtained. In Figure 4a, for $f < 90$ kHz, we obtain a drift rate of $f_d = -4.4$ kHz/s with $\sigma = 1.5$ and a probably error of ~1 kHz/s. In Figure 4b, $125 < f < 215$, $f_d = -5.7$ kHz/s with $\sigma = 2.7$ and a probably error of ~1.8 kHz/s. Finally, for Figure 4c, $250 < f < 340$ kHz, $f_d = -4.9$ kHz/s with $\sigma = 2.4$ and a probably error of ~1.6 kHz/s. In Table 1 we list the occurrence rate of striations found in the three frequency ranges. The occurrence frequency is defined as the ratio of the time when striations were observed to the total sampling time for a specific frequency range.

4. Drift Rate Analysis

In an effort to understand the generation of the fine structure striations, we first consider a motion of the AKR source region along the magnetic field line. Thus, in analogy to *Gurnett and Anderson* [1981], we consider a gyroresonant source of emission in a dipole magnetic field at a small polar angle such that

$$f_{ce} = k\,\mu_o / r^3 \text{ (Hz)}, \tag{1}$$

where $k = 5.6 \times 10^6$, r is the radial distance, and μ_o is the magnetic moment (Gauss-cm^3). Therefore

$$df_{ce}/dt = -3kBo\ dr/dt\ /\ r^4 \tag{2}$$

$$df_{ce}/dt = -3f_{ce}\ dr/dt\ /\ r. \tag{3}$$

For a gyroresonant source region drifting along the magnetic field line, df_{ce}/dt may be interpreted as a measure of the slope of the stripe on an f-versus-time spectrogram. Let us now define the ratio of df_{ce}/dt at two different radial distances, r_1 and r_2, as s, so that

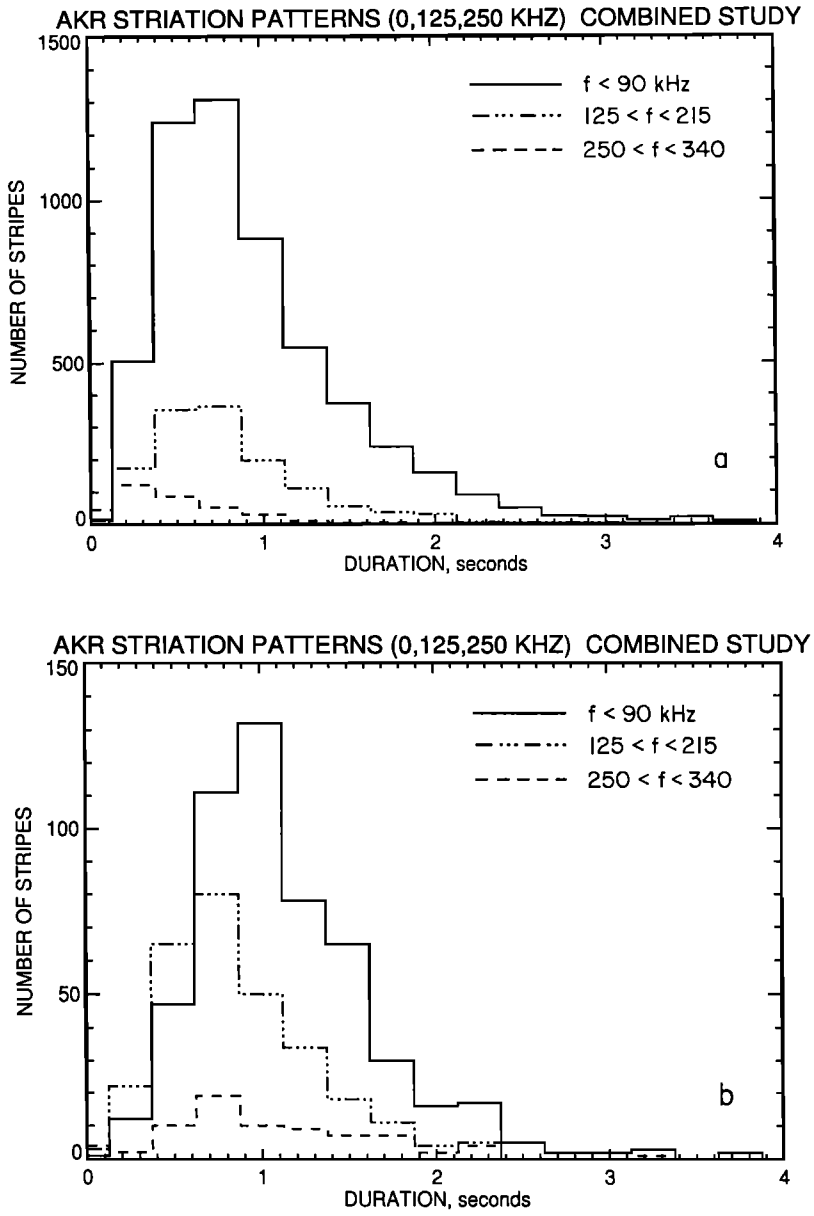

Figure 3. Distribution of the number of striations as a function of the duration in seconds for (a) negative and (b) positive slope striations. Data for bandwidths 0-90, 125-215, and 250-340 kHz are included. Most striations have a duration of less than 2 s, with a pronounced peak in the duration distribution between 0.5 and 1 s.

$$s = [df_{ce}/dt]_1/[df_{ce}/dt]_2 \quad (4)$$

or

$$s = [(f_{ce})_1 r_2 (dr/dt)_1]/[(f_{ce})_2 r_1 (dr/dt)_2] . \quad (5)$$

We choose $(f_{ce})_1 \sim 170$ kHz, $r_1 \sim 13{,}411$ km and $(f_{ce})_2 \sim 75$ kHz, $r_2 \sim 17{,}615$ km, obtaining $s \sim 2.98\ \alpha$, where $\alpha = [dr/dt]_1/[dr/dt]_2$. These frequencies were chosen as characteristic, midrange values for the two most important base frequencies of the wideband receiver, in the 90-kHz bandwidth mode. For a base frequency of 0 Hz, with AKR typically occurring for $f > 50$ kHz, 75 kHz is a nominal value. For a base frequency of 125 kHz, 170 kHz is a nominal, midrange value. To obtain a characteristic value for the parameter s, we use the results of the calculated frequency drift rates from Figures 4a and 4b to obtain $s \sim 1.3$ and $\alpha \sim 0.44$. The probable errors for the statistical drift rates are large, particularly for Figure 4b, used for $f = 170$ kHz. However, unless the drift rates for $f = 170$ kHz are significantly higher, i.e., $s > 3$, α will be less than 1. Such large values of s are highly unlikely even given the large probable errors of the Gaussian fits for Figures 4a and 4b.

This indicates that the stimulator of the striations must have an increasing velocity up the magnetic field line. This would seemingly rule out stimulation of the AKR striations by an upward traveling EMIC wave, because we would expect the group velocity of an EMIC wave to decrease as it propagates upward through the AKR source region, especially as it approaches the local ion cyclotron frequency. However, EMIC waves with decreasing velocities away from the Earth cannot be absolutely ruled out. The group velocity depends critically on many parameters including electron and ion density and the proximity of the wave frequency to the ion cyclotron frequency. From (3), at a frequency of 75 kHz,

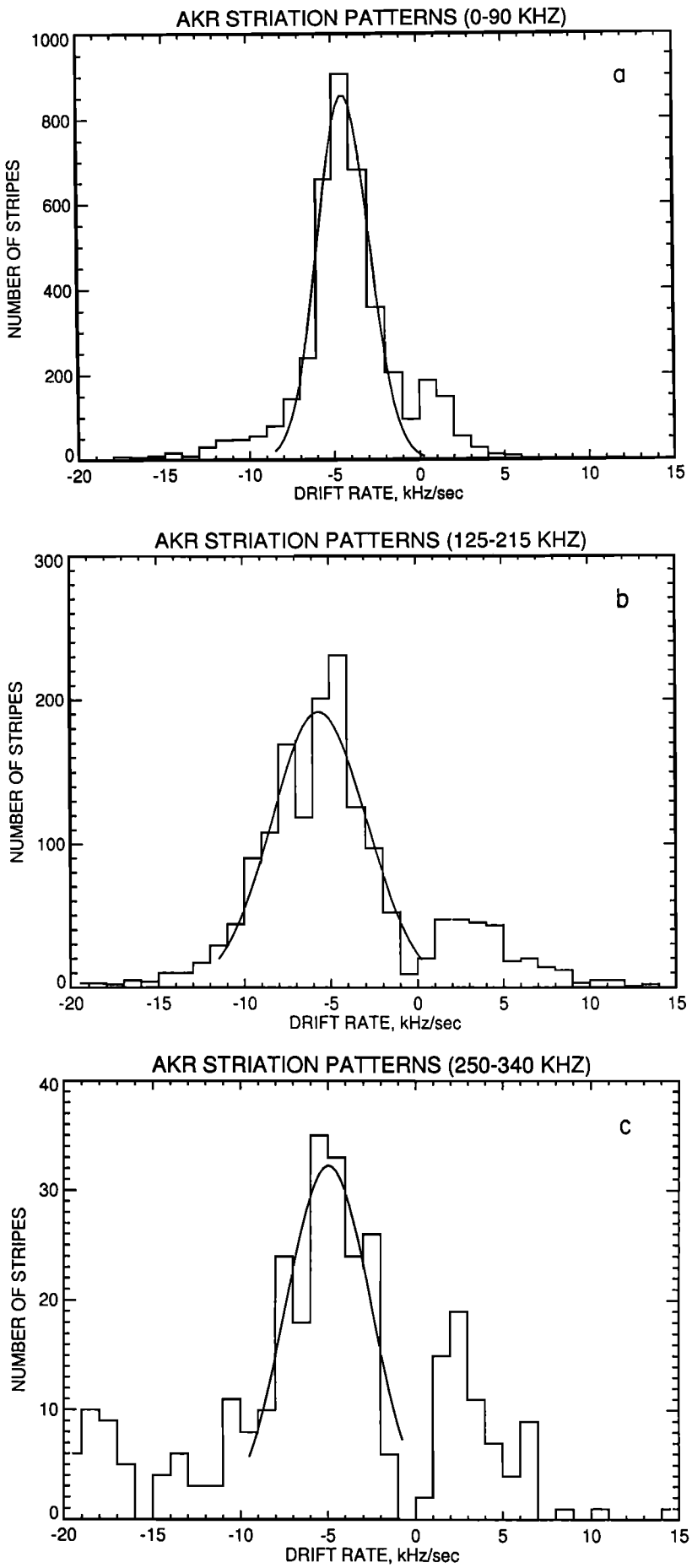

Figure 4. The distribution of the frequency drift rates of the AKR striations. We have further segmented the data according to frequency range: (a) 0-90 kHz; (b)125-215 kHz; and (c) 250-340 kHz. The data have been grouped in bins of 0.5 kHz/s.

Table 1. Occurrence Frequency of Striations for Survey 2

Frequency Range, kHz	*t/T*	Percent
0-90	1.53/13.3	11.5
125-215	0.86/8.33	10.4
250-340	0.39/15.9	2.4

The ratio *t/T* = time of observation (hours) to sampling time (hours).

$r \sim 17{,}615$, we obtain $[dr/dt]_1 \sim 340$ km/s. For $f \sim 170$ kHz, $r \sim 13{,}411$ km, we obtain $[dr/dt]_2 \sim 149$ km/s. These velocities are typical of ion beams that are accelerated upward by the upward electric fields of the auroral region with an energy of about 611 and 116 eV, respectively. Ion beams of these energies were commonly encounterd by DE 1 [cf. *Lin et al.*, 1985]. This has also been pointed out by *Strangeway et al.* [1999] using FAST observations within the auroral region. Ion beams would also be accelerated upward within the electric field of the acceleration region.

5. Summary

In an effort to determine the source of a unique class of AKR fine structure we call striations, we have conducted two surveys of the PWI plasma wave wideband (high resolution) receiver data. In survey 1 we randomly sampled wideband data during the entire first year of Polar operations. Since this survey included only a very small sample of data for $f > 90$ kHz, a second comprehensive survey of data was conducted during the first week of Polar operations, when PWI evenly sampled emissions over its entire frequency range.

These surveys of the PWI wideband receiver data from the Polar spacecraft have led to the determination that AKR fine structure patterns with very narrowband, negative drifting stripes occur in ~6.6% of the high-resolution wideband spectrograms. Since fine structure is essentially always present in AKR wideband data, this is equivalent to saying that the striations occur in ~6.6% of the fine structure data. The stripes are predominantly found in the 40- to 215-kHz frequency range (Table 1). Often occurring in groups or packets and sometimes in isolation, the striations appear to have a predominately negative linear slope, but with a significant number of positive slopes and a very narrow width $\Delta f/f$. Often fainter than the background AKR spectrum, the stripes are most easily identified extending below the frequency band of the more diffuse AKR spectral features.

More than 8200 AKR stripes from the combined survey 1 and survey 2 have been scaled to determine the physical characteristics of these very discrete features. We have found that the stripes have a frequency extent of about 4 kHz (for negative slopes) and a typical time duration of less than 2 s. The majority of the stripes display a negative slope in the range $-6 < R < -4$ kHz/s, with a peak near -4.4 kHz/s. Because of the limitations of the operating mode of the instrument (25% duty cycle), we can only place an upper limit on the width of an individual stripe at $\Delta f/f \sim 4 \times 10^{-3}$. However, the observed AKR fine structures probably have bandwidths much less than this.

Equation (3) is based on a simple model for the stimulation of AKR near the gyrofrequency. Using a value $df/dt = -4.4$ kHz/s (Figure 4a) and $f = 75$ kHz, we find $dr/dt \sim 340$ km/s. As shown by *Menietti et al.* [1996], such a velocity is compatible with an EMIC wave in the auroral region, and such an upward propagating wave was suggested as the stimulator of AKR and the source of the striations. However, our results indicate that there is only a weak increase in the measured slope of the striations with increasing frequency ($s \sim 1.3$), and this requires an increase in dr/dt, the velocity of the wave stimulator, with altitude (see equation (5)). This may be inconsistent with upward propagating EMIC waves, which are expected to decrease in velocity with height at altitudes of the AKR source region.

A velocity of ~400 km/s is not atypical of upward traveling ion beams within and above the auroral acceleration region. For completeness we note that upward auroral electrons typically have much higher velocities (~15,000 km/s) and do not appear to be the source of the observed AKR striations frequency drifts, even though upward electrons are proposed by *Carr and Reyes* [1999] to explain Jovian S-bursts. At present we know of no particular mechanism that would result in the stimulation of AKR by an upward traveling ion beam. Clearly, AKR striations are not present on every pass of the auroral region, while upward accelerated ion beams typically are. There may be special conditions, as yet undiscovered, which make possible the stimulation of AKR by upward traveling ion beams. The presence of a small but significant number of striations with positive slope must also be explained.

Recent observations of large-amplitude solitary structures in the downward current regions of the auroral zone [*Ergun et al.*, 1998a] suggest a possible alternative explanation for AKR striations. These solitary structures are described as electron holes traveling antiearthward with velocities that are a significant fraction of the particle beam (between ~500 and 5000 km/s). These velocities are of similar magnitude and direction as required to explain the AKR striation frequency drift rates. AKR is known to be generated in the upward current region, adjacent to the downward current region. Nevertheless, we believe the role of electron holes in the generation of AKR fine structure signatures is worthy of future investigation.

Acknowledgments. We thank J. Hospodarsky for typesetting the manuscript and R. L. Brechwald and J. H. Dowell for plots of the waveform data. We have benefitted greatly from many discussions of this analysis with Robert Strangeway and Amitava Bhattacharjee. This work was funded by NASA grant NAG5-7943.

Janet G. Luhmann thanks Simon G. Shepherd and Thomas D. Carr for their assistance in evaluating this paper.

References

Benson, R. F., M. M. Mellott, R. L. Huff, and D. A. Gurnett, Ordinary mode auroral kilometric radiation fine structure observed by DE-1, *J. Geophys. Res.*, *93*, 7515, 1988.

Calvert, W., A feedback model for the source of auroral kilometric radiation, *J. Geophys. Res.*, *87*, 8199, 1982.

Carr, T. D., and F. Reyes, Microstructure of Jovian decametric S bursts, *J. Geophys. Res.*, *104*, 25,127, 1999.

Carr, T. D., M. D. Desch, and J. K. Alexander, Phenomenology of magnetospheric radio emissions, in *Physics of the Jovian Magnetosphere*, edited by A. J. Dessler, pp. 226-284, Cambridge Univ. Press, New York, 1983.

Carr, T. D., K. Imai, L. Wang, L. Garcia, F. Reyes, C. H. Higgins, and W. B. Greenman, Recent results by the University of Florida group from low frequency radio observations of Jupiter and Neptune, in *Planetary Radio Emissions IV*, edited by H. O. Rucker, S. J. Bauer, and A. Lecacheux, pp. 25-41, Austrian Acad. of Sci. Press, Vienna, Austria, 1997.

Delory, G. T., R. E. Ergun, C. W. Carlson, L. Muschietti, C. C. Chaston, W. Peria, J. P. McFadden, and R. Strangeway, FAST observations of electron distributions within AKR source regions, *Geophys. Res. Lett.*, *25*, 2069, 1998.

Ergun, R. E., et al., FAST satellite observations of large-amplitude solitary structures, *Geophys. Res. Lett.*, *25*, 2041, 1998a.

Ergun, R. E., et al., FAST satellite wave observations in the AKR source region, *Geophys. Res. Lett.*, *25*, 2061, 1998b.

Farrell, W., Fine structure of auroral kilometric radiation: A Fermi acceleration process?, *Radio Sci.*, *30*, 961, 1995.

Grabbe, C. L., Theory of fine structure of auroral kilometric radiation, *Geophys. Res. Lett.*, *9*, 155, 1982.

Grabbe, C., K. Papodopoulos, and P. Palmadesso, A coherent nonlinear theory of auroral kilometric radiation, 1, Steady state model, *J. Geophys. Res.*, *85*, 3337, 1980.

Gurnett, D. A., and R. R. Anderson, The kilometric radio emission spectrum: Relationship to auroral acceleration processes, in *Physics of Auroral Arc Formation, Geophys. Monogr. Ser.*, Vol. 25, edited by S.-I. Akasofu and J. R. Kan, pp. 341-350, AGU, Washington, D. C., 1981.

Gurnett, D. A., R. R. Anderson, F. L. Scarf, R. W. Fredericks, and E. J. Smith, Initial results from the ISEE 1 and 2 plasma wave investigation, *Space Sci. Rev.*, *23*, 103, 1979.

Gurnett, D. A., et al., The Polar plasma wave instrument, *Space Sci. Rev.*, *71*, 597, 1995.

Helliwell, R. A., A theory of discrete VLF emissions from the magnetosphere, *J. Geophys. Res.*, *72*, 4773, 1967.

Kellogg, P. J., and S. J. Monson, Radio emissions from the aurora, *Geophys. Res. Lett.*, *6*, 297, 1979.

LaBelle, J., M. L. Trimpi, R. Brittain, and A. T. Weatherwax, Fine structure of auroral ROAR emissions, *J. Geophys. Res.*, *100*, 21,953, 1995.

Lin, C. S., J. N. Barfield, J. L. Burch, and J. D. Winningham, Near-conjugate observations of inverted V electron precipitation using DE 1 and DE 2, *J. Geophys. Res.*, *90*, 1669, 1985.

McKean, M. E., and R. M. Winglee, A model for the frequency fine structure of auroral kilometric radiation, *J. Geophys. Res.*, *96*, 21,055, 1991.

Melrose, D. B., A phase-bunching mechanism for fine structures in auroral kilometric radiation and Jovian decametric radiation, *J. Geophys. Res.*, *91*, 7970, 1986.

Menietti, J. D., H. K. Wong, W. S. Kurth, D. A. Gurnett, L. J. Granroth, and J. B. Groene, Discrete, stimulated auroral kilometric radiation observed in the Galileo and DE 1 wideband data, *J. Geophys. Res.*, *101*, 10,673, 1996.

Menietti, J. D., H. K. Wong, W. S. Kurth, D. A. Gurnett, L. J. Granroth, and J. B. Groene, Possible stimulated AKR observed in Galileo, DE-1, and Polar wideband data, in *Planetary Radio Emissions IV*, edited by H. O. Rucker, S. J. Bauer, and A. Lecacheux, pp. 259-273, Austrian Acad. of Sci. Press, Vienna, Austria, 1997.

Morioka, A., H. Oya, and S. Miyatake, Terrestrial kilometric radiation observed by satellite JIKKIKEN (EXOS-B), *J. Geomagn. Geoelectr.*, *33*, 37, 1981.

Pritchett, P. L., R. J. Strangeway, C. W. Carlson, R. E. Ergun, J. P. McFadden, and G. T. Delory, Free energy sources and frequency bandwidth for the auroral kilometric radiation, *J. Geophys. Res.*, *104*, 10,317, 1999.

Shepherd, S., J. LaBelle, M. Trimpi, and R. Brittain, Further investigation of auroral roar fine structure, in *Planetary Radio Emissions IV*, edited by H. O. Rucker, S. J. Bauer, and A. Lecacheux, pp. 291-292, Austrian Acad. of Sci. Press, Vienna, Austria, 1997.

Shepherd, S. G., J. Labelle, and M. L. Trimpi, Further investigation of auroral roar fine structure, *J. Geophys. Res.*, *103*, 2219, 1998.

Strangeway, R. J., P. L. Pritchett, R. E. Ergun, C. W. Carlson, J. P. McFadden, and G. T. Delory, Evidence that the fine structure of auroral kilometric radiation is not intrinsic to the source mechanism, paper presented at the International Union of Radio Science National Meeting, Boulder, Colo., Jan. 4-8, 1999.

Wu, C. S., and L. C. Lee, A theory of the terrestrial kilometric radiation, *Astrophys. J.*, *230*, 621, 1979.

Yoon, P. H., and A. T. Weatherwax, A theory for AKR fine frequency structure, *Geophys. Res. Lett.*, *25*, 4461, 1998.

Zarka, P., T. Farges, B. P. Ryabov, M. Abada-Simon, and L. Denis, A scenario for Jovian S-bursts, *Geophys. Res. Lett.*, *23*, 125, 1996.

D. A. Gurnett, J. D. Menietti, A. M. Persoon, and J. S. Pickett, Department of Physics and Astronomy, University of Iowa, 203 Van Allen Hall, Iowa City, IA 52242-1479. (jdm@space.physics.uiowa.edu)

(Received October 18, 1999; revised December 28, 1999;
accepted December 29, 1999.)